

Numerical Modeling and Simulations of Electrical Characteristics of Multi-layer Organic Light Emitting Diodes

Hyun Jung Lee[a], Yong Soo Lee*[b], Jae-Hoon Park**[c], and Jong Sun Choi*[d]**

Abstract

Theoretical simulations of spatial distribution of charge carriers and recombination rate, and J-V characteristics of the multi-layer organic light emitting diodes are carried out. Drift-diffusion current transport, field-dependent carrier mobility, exponential and Gaussian trap distribution, and Langevin recombination models are included in this computer model. The simulated results show good agreement with the experimental data confirming the validity of the physical models for organic light emitting diodes.

Keywords : OLED, Multilayer, Simulation

1. Introduction

The organic light emitting diodes based on the small molecules or conjugated polymers have been given much attention due to their possible applications in the flat panel displays. Many investigations have been carried out on the commercial applications, but some of the important electrical characteristics have not been identified yet.

Although the organic light emitting diodes have been intensively studied in the last decade, there is still much room both for further understanding the fundamental device physics and for improvement of device technologies. At this stage of development, the device simulation becomes very helpful in that it would help explain the various experimental results and also give insights on the device physics [1-5].

In this work, we have performed the numerical device simulation of the multi-layer organic light emitting diodes. The drift-diffusion current transport, the field-dependent carrier mobility, the trap distribution, and the recombination models are included in this computer model. The current-voltage characteristics and the spatial distribution of charge carrier concentration and the recombination rate in the device structure will be presented.

2. Models

The computer model for the organic light emitting diodes is based on the solution to the Poisson's equation and continuity equation for hole and electron:

$$\frac{d^2V}{dx^2} = -\frac{q}{\varepsilon_0\varepsilon_r}(p - n + N_t) \tag{1}$$

$$\frac{dJ_n}{dx} = q(R_n - G_n) \tag{2}$$

$$\frac{dJ_p}{dx} = -q(R_p - G_p) \tag{3}$$

The hole and electron currents are given by the drift-diffusion transport equation:

$$J_n = kT\mu_n \frac{dn}{dx} - q\mu_n n\frac{dV}{dx} \tag{4}$$

$$J_p = -kT\mu_p \frac{dp}{dx} - q\mu_p p\frac{dV}{dx} \tag{5}$$

Manuscript received August 11, 2007; accepted for publication September 15, 2007.
This work was supported from Seoul Research and Business Development (Seoul R&BD) Program (10555).
* Member, KIDS; ** Student Member, KIDS
Corresponding Author : Hyun Jung Lee
[a]Dept. of Electrical, Information & Control Engineering, Hongik University
72-1, Sangsu-dong, Mapo-gu, Seoul, 121-791, KOREA
[b]Samsung SDI
428-5, Gongse-dong, Giheung-gu, Yongin-si, Gyeonggi-do, 446-577, KOREA
[c]Research Institute of Information Display, Hanyang University
17, Haengdang-dong, Seongdong-gu, Seoul, 133-791, KOREA
[d]Dept. of Electrical, Information & Control Engineering, Hongik University
72-1, Sangsu-dong, Mapo-gu, Seoul, 121-791, KOREA
E-mail : runy0508@naver.com **Tel** : 02-320-3097 **Fax** : 02-320-1110

where V is the potential, ε_0 and ε_r are the permittivity of the free space and relative permittivity, $p(n)$ is the hole(electron) density, N_t is the charge trapped in the organic layer bulk, q is the elementary charge, $R_{p(n)}$ is the charge carrier recombination rate for hole(electron), $G_{p(n)}$ is the charge carrier generation rate for hole(electron), $J_{p(n)}$ is the hole(electron) current density, k is the Boltzmann constant, T is the temperature, and $\mu_{p(n)}$ is the hole(electron) mobility. The generation rates for hole and electron were assumed to be negligible because of the insulator-like properties of the organic materials. The diffusion coefficient could be expressed by Einstein the relationship with the charge carrier mobilities[6].

The charge carrier mobilities are expected to be field-dependent in amorphous organic materials for organic light emitting diodes and thus were modeled as follows [1, 2]:

$$\mu = \mu_0 \exp\sqrt{\frac{E}{E_0}} \tag{6}$$

where μ_0 and E_0 are the organic material parameters and E the electric field.

The multi-layer organic light emitting diodes have an internal interface at organic-organic interface. The thermionic emission current and a backflowing interface recombination current were used to model the internal interface [3, 4]. In order to achieve high performance organic light emitting diodes, ohmic contacts for hole and electron injection are required [5]. Ohmic boundary conditions were assumed at the carrier injecting contacts.

The distribution of the band tail states was assumed to have an exponential energy dependence. The valence band tail and the conduction band tail were assumed to be donor-like and acceptor-like, respectively. The charge trapped in the exponential tail states is given by [6]

$$N_t = \int_{E_V}^{E_C} [(1 - f_D(E))g_D(E) - f_A(E)g_A(E)]dE \tag{7}$$

where the occupation statistics are given by

$$f_D(E) = \frac{c_{nd}n + c_{pd}N_V e^{(E_V - E)/kT}}{c_{nd}(n + N_C e^{(E - E_C)/kT}) + c_{pd}(p + N_V e^{(E_V - E)/kT})} \tag{8}$$

$$f_A(E) = \frac{c_{na}n + c_{pa}N_V e^{(E_V - E)/kT}}{c_{na}(n + N_C e^{(E - E_C)/kT}) + c_{pa}(p + N_V e^{(E_V - E)/kT})} \tag{9}$$

where c_{nd} and c_{pd} are the capture cross-sections in the conduction band tail for electrons and holes respectively, and c_{na} and c_{pa} are the capture cross-sections in the valence band tail for electrons and holes respectively. The $g_D(E)$ is the donor-like density of the valence band tail states and the $g_A(E)$ is the acceptor-like density of the conduction band tail states. N_V and N_C are the effective densities of states for the valence and conduction bands.

The recombination rate was modeled by the Langevin recombination theory. If the holes and electrons are statistically independent of each other, the carrier recombination is a random process and is kinetically bimolecular [7]. The recombination model is given by

$$R = \frac{q}{\varepsilon_0 \varepsilon_r}(\mu_n + \mu_p)pn \tag{10}$$

The highly non-linear nature of the transport equations to be solved suggested the use of approximate numerical methods. The well-known finite-difference method was chosen for simplicity and accuracy. Since the dependent variables (v, n, p) in the above equations are of greatly different orders of magnitude and show a very different behavior in regions with the space charge, the first step in conducting a structural analysis of the above equations is an appropriate normalization [8]. The discretized equations were normalized by A. de Mari scheme [9]. For the discretization at the internal interface nodes, the Sutherland algorithm was used [10]. The damping method was used to prevent the abrupt change by large steps when the high bias is applied.

3. Results and discussion

The simulated and measured current-voltage characteristics are shown in Fig. 1, where the data in a semi-logarithmic scale is inserted. The fabricated device has an acid treated- ITO/TPD/Alq_3/Li:Al structure. The thicknesses of the organic layers for the devices are 50nm, respectively. The μ_{p0} of the hole transport layer (HTL), the other zero-field mobility parameters, and the E_0 were chosen as 1×10^{-3} cm^2/Vs, 1×10^{-6} cm^2/Vs, and 3×10^4 V/cm, respectively, to ensure a good agreement between simulated and measured results.

The sensitivity simulation results of the current-voltage characteristics and the recombination rate profile to

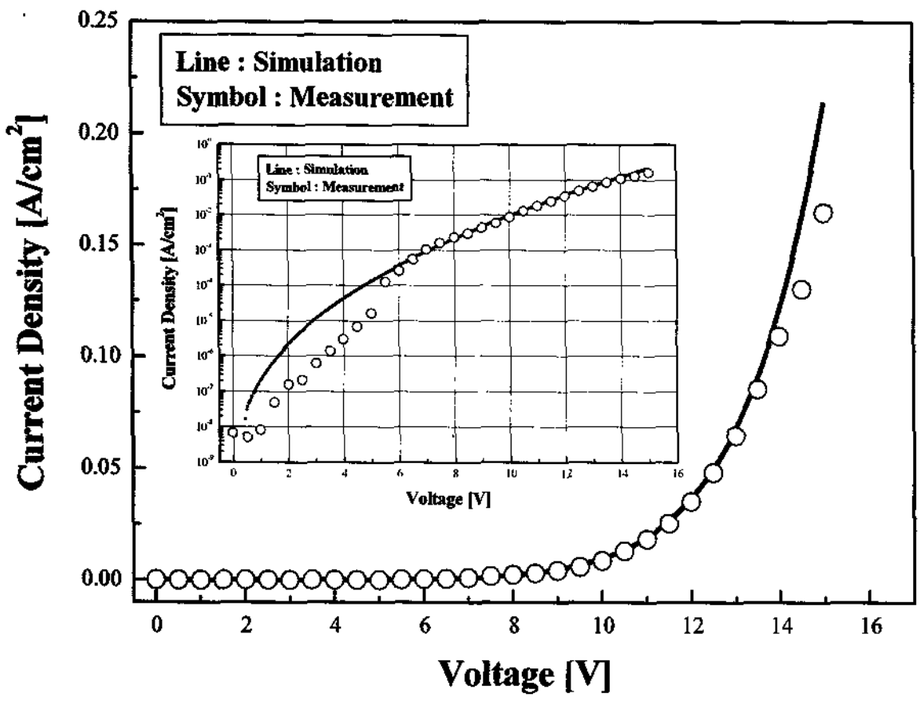

Fig. 1. Simulated and measured current-voltage characteristics, inset; a semi-logarithmic data.

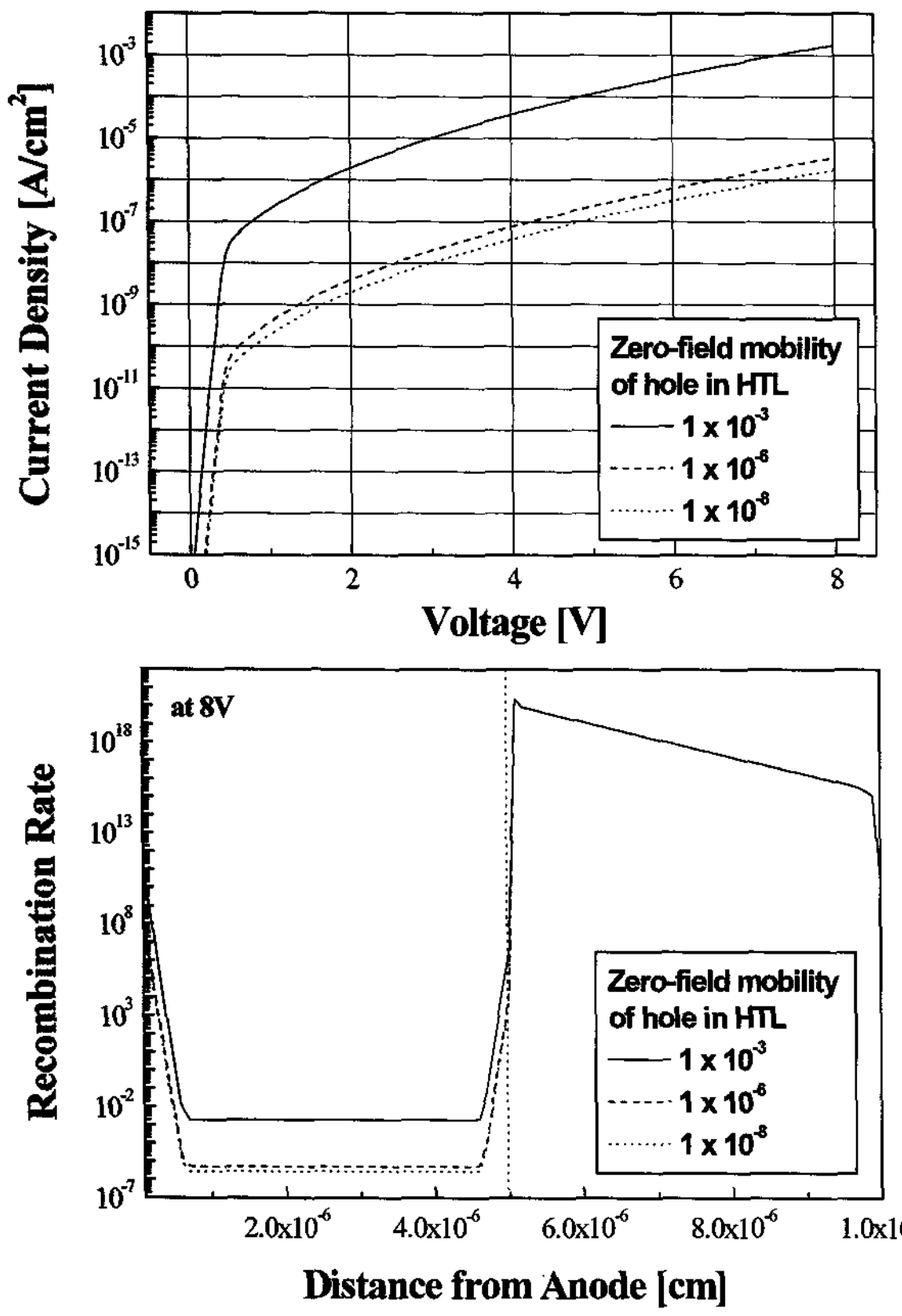

Fig. 2. Current density-voltage characteristics and recombination rate profile with variety zero-field hole mobilities of HTL.

the zero-field hole mobility of the HTL are shown in Fig. 2. In the upper panel of the figure, the different values of the hole mobility of the HTL provides distinctly different current-voltage characteristics, which indicates that the holes of the HTL is the dominant charge transporting carrier of the bilayer organic light emitting diodes.

The simulation results show that the variation of the hole mobility, however, has negligible effect on the recombination rate distribution in the ETL side. This is due to the low barrier height for hole (0.3 eV) between the valence band of the HTL and the valence band of the ETL in the TPD-Alq_3 bilayer structure, which can let the holes pass through the barrier. The simulated current density-voltage characteristics and the recombination rate profile with various zero-field electron mobilities of the ETL are shown in Fig. 3. The current density-voltage characteristics are almost independent of the electron mobility of the ETL, but the recombination rate in the ETL side varies with the electron mobility of the ETL. The higher recombination rate is obtained with the higher electron mobility.

The calculated recombination rate exhibited nearly invariable distribution over a whole ETL with very low electron mobility (1×10^{-10} cm^2/Vs). The low electron mobility causes the electrons of the ETL to meet with the fast holes, which have passed through the HTL-ETL interface barrier, at the vicinity of the electron injecting

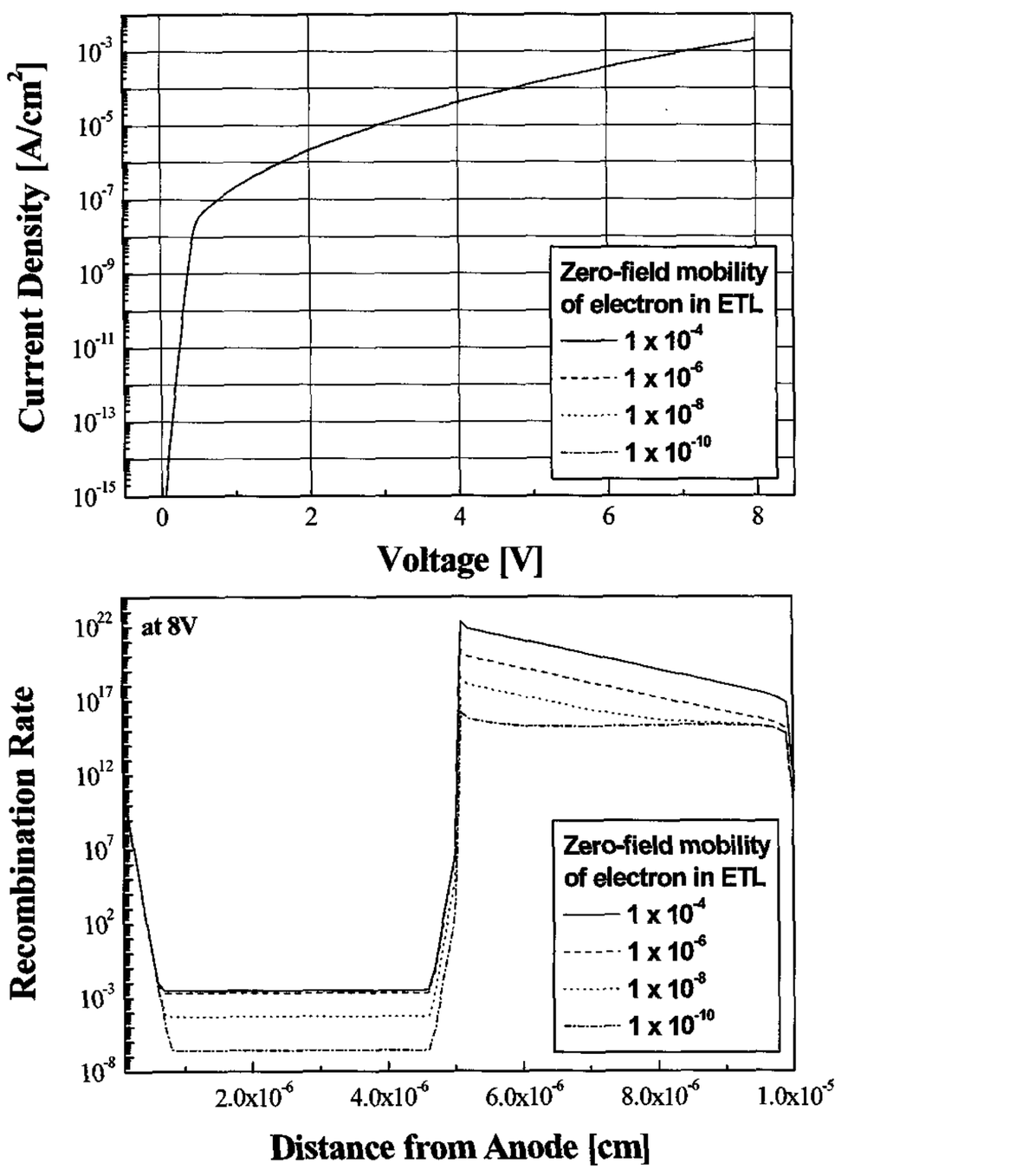

Fig. 3. Current density-voltage characteristics and recombination rate profile with variety zero-field electron mobilities of ETL.

contact. For this case, most of the recombination are non-radiative, which reduces the device efficiency due to the unbalanced hole and electron distributions [4].

To improve the charge carrier injection from the electrodes into the organic semiconductor is a challenge for designing efficient OLEDs. In general, because the contact between the ITO and the HTL materials is non-ohmic, [and thereby for the enhanced carrier injection, the hole injection layer (HIL) between the anode and HTL layer is commonly used.

The simulated and measured J-V characteristics of the bilayer and triple-layer OLEDs are compared in Fig. 4. The fabricated triple-layer OLEDs have the ITO/α-septithiophene (α-7T)/TPD/Alq_3/composite cathode structure, where the α-7T layer plays a role of the HIL [11-12], whose molecular is shown in the inset of Fig. 4. The low work function metal materials have been used as a cathode to improve the electron injection into OLEDs.

However, OLEDs using low work function metal cathodes exhibited inferior stability. In order to ohmic contact model at the cathode-organic layer interface, a composite cathode was used. The co-evaporated cathode, such as alkaline metals (CsF, KF, and NaF) and Al co-evaporation, is applied to enhance OLEDs performances and stability. Especially, CsF can be thermally deposited at lower temperature compared with LiF so that the exposure of the organic layers to the heat during the evaporation of the metals can be avoided [13].

By using the HIL and composite cathode, the anode/cathode-organic layer contacts could be formed and modeled as effectively ohmic. The zero-field hole mobilities of the HIL and HTL were chosen as 1×10^{-3} $cm^2/V \cdot sec$, the other zero-field mobilities were chosen as 1×10^{-6} $cm^2/V \cdot sec$, and the hole internal barrier height at the HIL-HTL interface was set to be 0.4 eV, to obtain the best fit of the simulated results to the measured results. When the α-7T layer was used as the HIL, the turn-on voltage of the device was lowered compared with that of the device without the HIL due to the enhanced hole injection through the lowered injecting barrier at the ITO/TPD boundary and improved hole transport.

The simulated charge carrier concentrations and the recombination rate profiles of the triple-layer structure OLEDs are shown in Fig. 5 and 6. The accumulated hole concentration was obtained at the HIL-HTL interface and the recombination rate of the triple-layer structure OLEDs was much higher than that of the double-layer due to the

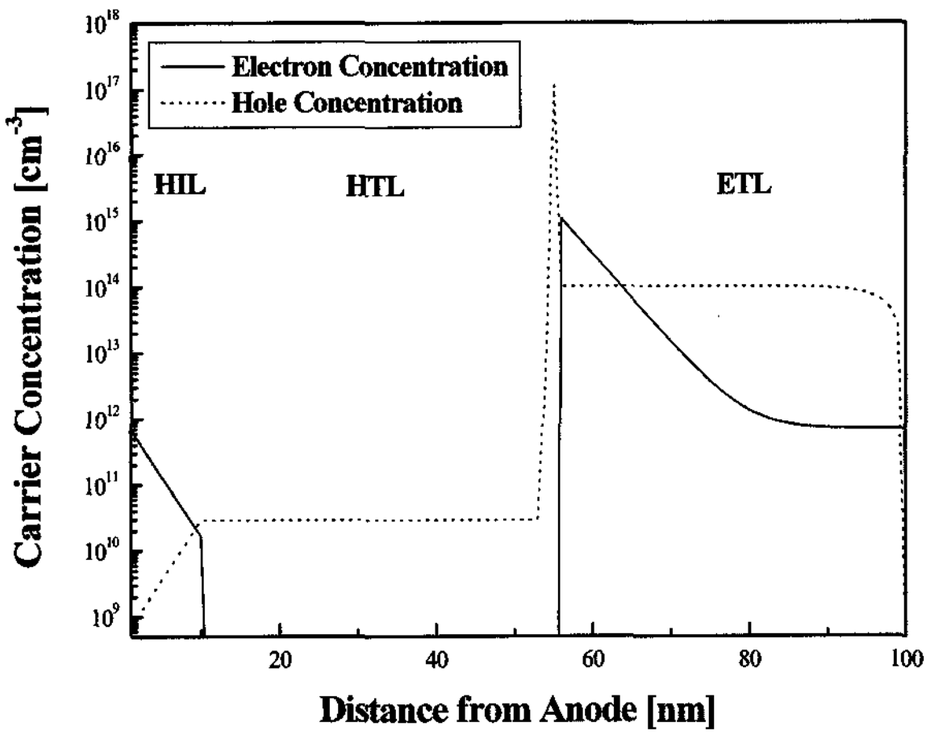

Fig. 5. Spatial distribution profile of the charge carriers concentrations.

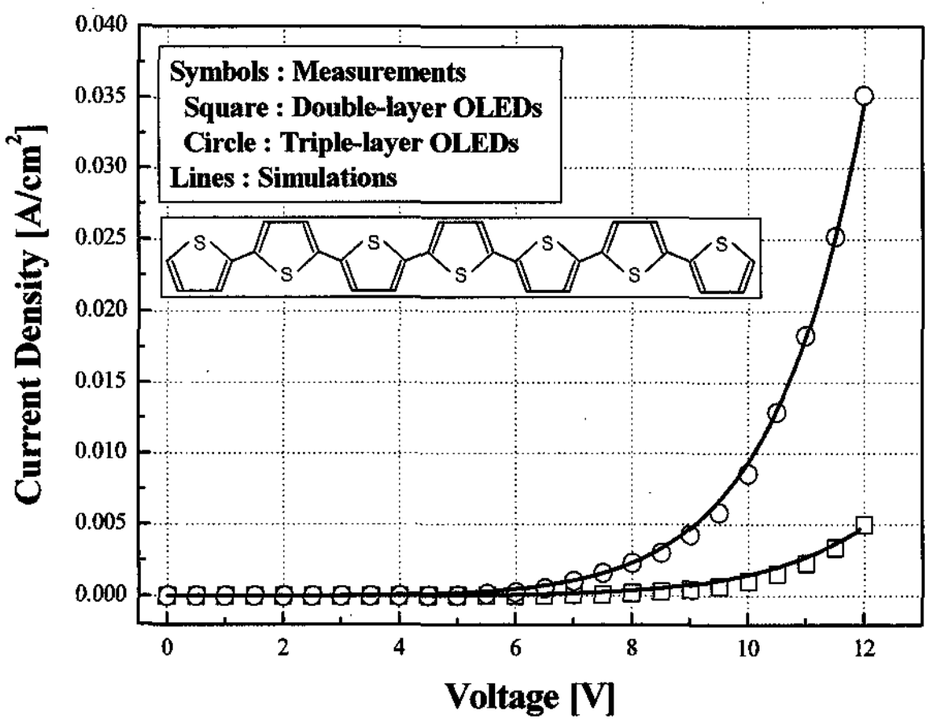

Fig. 4. Measured and simulated current-voltage characteristics, inset: the molecular structure of α-7T.

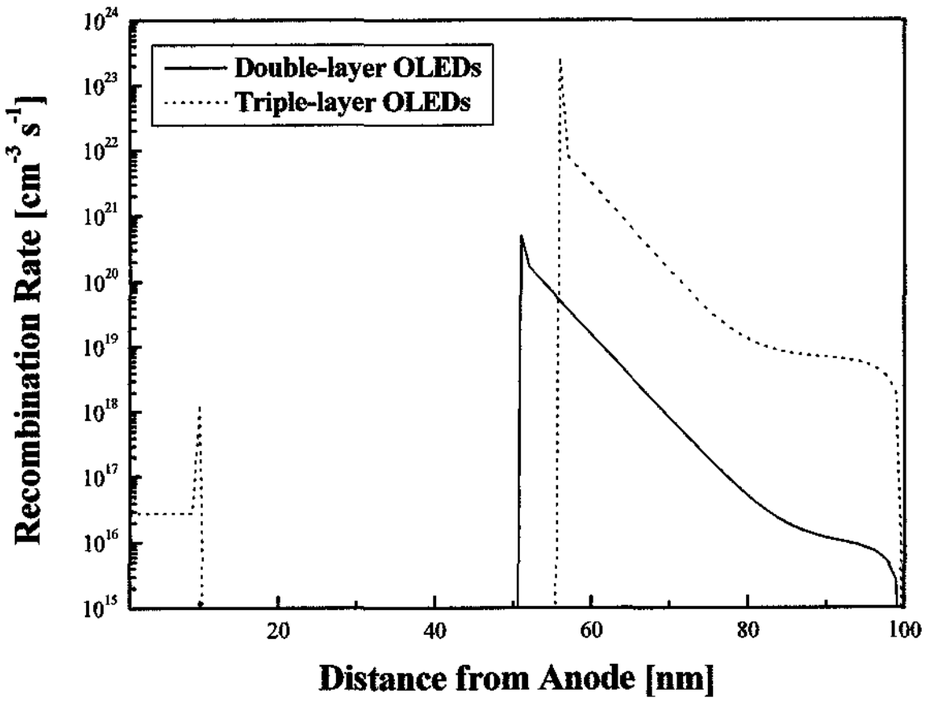

Fig. 6. Recombination rates profile of ITO/α-7T/TPD/Alq_3/composite cathode

improved carrier injection efficiency as shown in Fig. 6, which is consistent with the previous experimental results [11]. The variations of the simulated current densities and the maximum recombination rates for different hole mobilities of HIL are also shown in Fig. 7. The current densities and the recombination rates are independent of the hole mobilities of the HIL.

The device characteristics of the triple-layer OLEDs with copper phthalocyanine (CuPc) HIL were simulated, and the simulated and measured J-V characteristics are shown in Fig. 8, where the J-V characteristics of the ITO/TPD/Alq_3/Li:Al device is compared with that of the ITO/CuPc/TPD/ Alq_3/Li:Al device. The triple-layer OLEDs with the CuPc HIL provides much improved J-V characteristic compared with that of the double-layer device. This is due to the improvement in the hole transport by the HIL employment.

The calculated recombination rate profile of the triple-layer device including CuPc HIL is shown in Fig. 9. The recombination rate of the triple-layer OLEDs is about two orders of magnitude greater than that of the double-layer OLEDs. This is due to the improvement of the carrier injection efficiency. The various parameters for the simulations of both triple-layer devices (both with α-7T and CuPc) are shown in Table 1.

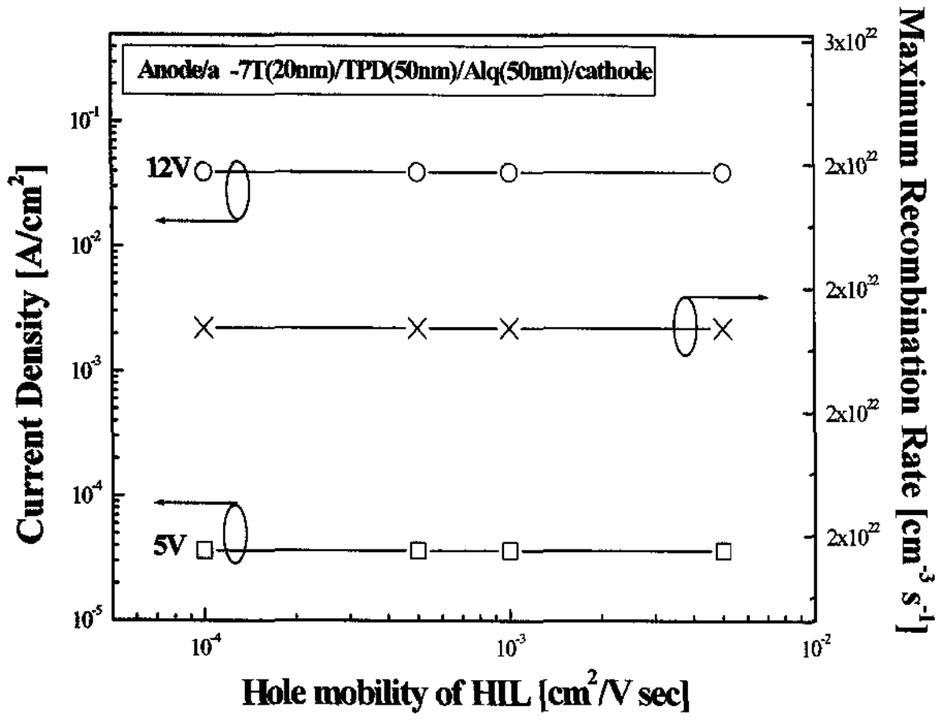

Fig. 7. Variations of the simulated current densities and the maximum recombination rates for different hole mobilities of HIL.

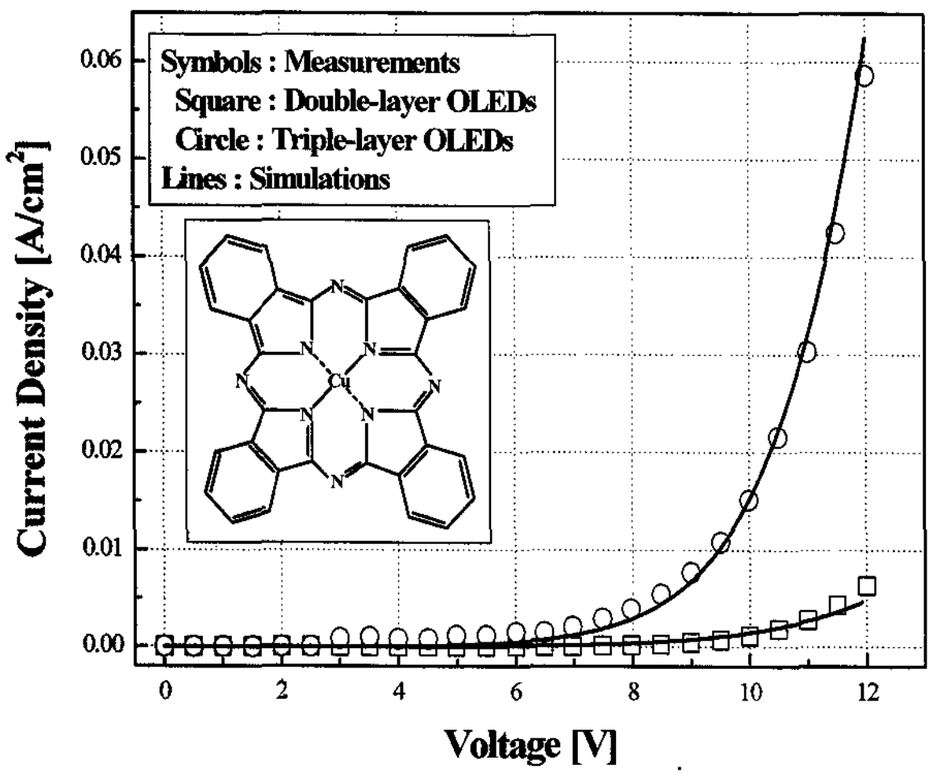

Fig. 8. Measured and simulated current density-voltage characteristics, inset: the molecular structure of CuPc.

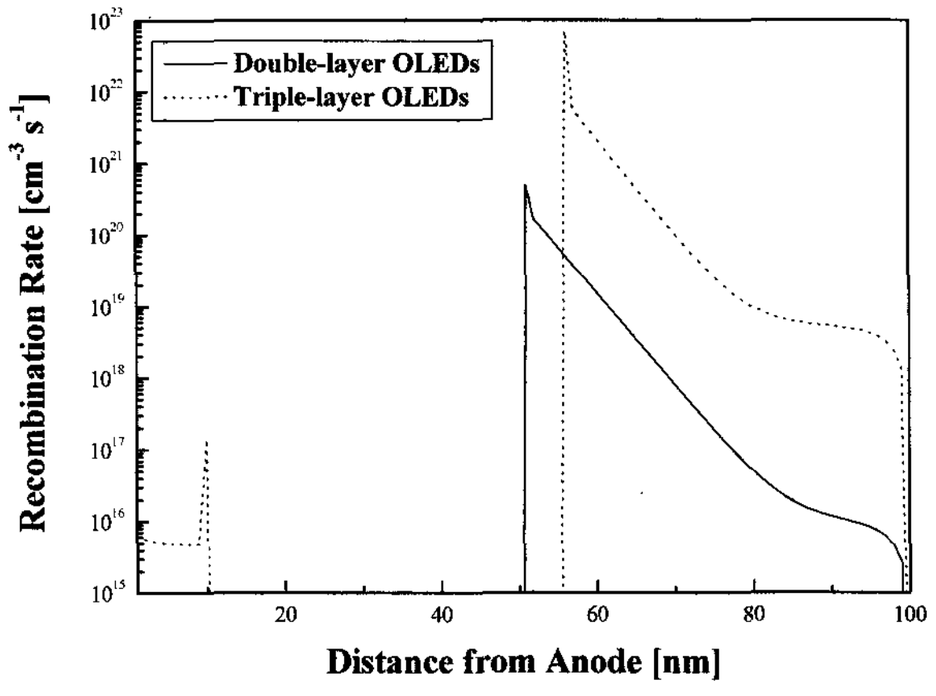

Fig. 9. Recombination rates profile of ITO/CuPc/TPD/Alq_3/Li:Al.

Table 1. Parameters for simulations of ITO/α-7T/TPD/Alq_3/Al-CsF and ITO/CuPc/TPD/Alq_3/Li:Al structures.

Parameters	α -7T HIL use	CuPc HIL use
Anode/cathode contacts model	Ohmic	Ohmic
E_G of HIL	2.3 eV	1.7 eV
Φ_h at HIL/HTL	0.4 eV	0.3 eV
E_0	2.0×10^5 V/cm	2.2×10^5 V/cm
μ_{p0i} & μ_{p01}	1.0×10^{-3} cm^2/Vs	
The other mobilities	1.0×10^{-6} cm^2/Vs	
Thickness of HIL	10 nm	
Thickness of HTL	45 nm	
Thickness of ETL	45 nm	

4. Conclusions

The numerical device model for the OLEDs was presented. The electrical characteristics of the double-layer OLEDs were calculated and the results have best fit to the measured data. The computer model was applied to simulate the electrical characteristics of the triple-layer OLEDs which showed that the J-V characteristics of the devices can be governed by using the hole injection control at the anode-HTL interface. The simulation characteristics of the triple-layer OLEDs including α-7T and CuPc HIL were also discussed. Although the complicated and interrelated nature of the organic material parameters made it quite difficult to predict their exact and realistic values, the optimized parameter values were quite reasonable and the validity of the computer model was confirmed and could be adopted to design and analyze the OLED devices.

References

[1] P.W.M. Blom and J.M. de Jong, IEEE J. Selected Topics in Quantum Electronics, **4**, 105 (1998).
[2] Y.N. Gartstein and E.M. Conwell, Chem. Phys. Lett., **245**, 351 (1995).
[3] P.S. Davids, I.H. Campbell, and D.L. Smith, J. Appl. Phys., **82**, 6319 (1997).
[4] B.K. Crone, P.S. Davids, I.H. Campbell, and D.L. Smith, J. Appl. Phys., **87**, 1974 (2000).
[5] J. Staudigel, M. Stößel, F. Steuber, and J.Simmerer, J. Appl. Phys., **86**, 3895 (1999).
[6] J.S. Choi, Ph. D. Thesis, Purdue University (1992).
[7] M. Pope and C.E. Swenberg, Electronic Processes in Organic Crystals, (Oxford University Press, New York, 1982), p.958
[8] S. Selberherr, Analysis and Simulation of Semiconductor Devices, (Springer-Verlag, Wien, New York, 1984).
[9] A. de Mari, Solid-State Electronics, **11**, 33 (1968).
[10] A.D. Sutherland, Solid-State Electronics, **23**, 1085 (1980).
[11] J. H. Park, Y. Lee, and J. S. Choi, J. Information Display, **4**, 19 (2003).
[12] S. T. Lim and D. M. Shin, Synth. Metals, **117**, 229 (2001).
[13] G. E. Jabbour, B. Kippelen, N. R. Armstrong, and N. Peyghambarian, Appl. Phys. Lett. **73,** 11 (1998).